Mechatronics xxx (2014) xxx–xxx

Contents lists available at ScienceDirect

Mechatronics

journal homepage: www.elsevier.com/locate/mechatronics

A task oriented haptic gait rehabilitation robot

K.J. Chisholm, K. Klumper, A. Mullins, M. Ahmadi *

Department of Mechanical and Aerospace Engineering, Carleton University, Ottawa, ON K1S 5B6, Canada

ARTICLE INFO

Article history:
Received 6 October 2013
Accepted 6 July 2014
Available online xxxx

Keywords:
Robotics
Haptics
Design
Gait rehabilitation
Virtual environments
Rehabilitation robotics

ABSTRACT

This paper presents the concept, design process, and the prototype of a novel haptics-based lower-extremity rehabilitation robot for bed-ridden stroke patients. This system, named Virtual Gait Rehabilitation Robot (ViGRR), is required to provide the average gait motion training as well as other targeted exercises such as leg press, stair stepping and motivational gaming, in order to facilitate motor learning and enable the training of daily activities such as walking and maintaining balance. The system requirements are laid out and linked to the design of a redundant planar 4DOF robot concept prototype. An iterative design optimization loop was setup to obtain the robot kinematic and dynamic parameters as well as the actuators. The robot's mechanical design, model, safety features, admittance controllers, and the architecture of the haptic controller are presented. Preliminary experiments were planned and performed to evaluate the capability of the system in delivering task-based virtual-reality exercises and trajectory following scenarios.

1. Introduction

Rehabilitation robotics aims at developing novel technologies and associated protocols to assist therapists in serving an ever increasing elderly population and stroke victims [1]. Approximately 50,000 Canadians and 780,000 Americans suffer a stroke each year, resulting in disabilities, reduced mobility, independence, and quality of life [2,3]. Based on principles of motor learning and recovery, the current stroke rehabilitation practices focus on intensive, cognitively demanding, time-consuming and repetitive exercise regiments [4]. Early intervention is identified as critical for stroke patients and shown to improve functional outcomes [5,6].

Specialized gait rehabilitation robotics have the potential to provide improved functional gains for patients by incorporating high-intensity repetitive exercises over an extended period [1,7]. There are still many challenges on integrating robotics into a stroke rehabilitation intervention and questions regarding their efficacy and patient outcomes in the absence of clinically relevant data [8,9]. The current rehabilitation robotics mainly focuses on patients with partial load bearing or use of body weight support system, limiting their benefits in assisting bed-ridden patients. Carleton University's Advanced Biomechatronics and Locomotion laboratory (ABL) has developed the Virtual Gait Rehabilitation Robot (ViGRR), designed to work with bed-ridden patients and provide various activities including haptic sensation of ground reactions. ViGRR promises to develop new features which can add value to patients and therapists, and save on healthcare cost in stroke rehabilitation.

Gait rehabilitation robots primarily include body weight supported treadmill training where an exoskeleton guides the patient through a trajectory, thus alleviating the burden of therapists in manipulating the patients' legs [10,11]. The Lokomat [11] and other devices such as the Autoambulator [12] and Lokohelp [13] provided guided average gait training limited to sagittal plane floor walking. New technologies complement behaviour driven motor learning models that encourage the patient to initiate movements and provide assistance as-needed during exercise. The Lokomat now incorporates impedance control schemes that attempt to adapt to a patient's intentional changes in gait parameters such as cadence and stride length with modifiable assistance given by the robot [14]. The ALEX robot employs a force-tunnel control scheme to guide a patient through a desired foot trajectory to improve retention of skill development and motor learning [15,16]. For less resistance and more natural gait, LOPES incorporates extra degrees of freedom, lightweight compliant actuators, and impedance based virtual assistance models for gait training [17]. The WalkTrainer promises over-ground walking instead of using a treadmill, for a more realistic experience, and incorporating muscle stimulation [18].

In order to expand the capabilities of a robotic system beyond over-ground activities such as sit-to-stand or stair climbing, the HapticWalker [19,20] and G-EO-Systems trainer [21] employ a robot end effector interfaced with the patient's foot. These

* Corresponding author. Tel.: +1 613 520 2600x4057.
E-mail address: mojtaba.ahmadi@carleton.ca (M. Ahmadi).

http://dx.doi.org/10.1016/j.mechatronics.2014.07.001
0957-4158/

footplate-based robotic devices also allow free motion of the leg's joints so that there are no restrictive or unsafe interactions across the knee or hip that can result from cross-joint actuators with exoskeleton robots. Other footplate-based exercise machines do not include full gait trajectories, such as Erigo, incorporates foot pedals with physiological biofeedback mechanisms, e.g. heart rate and stress, to continuously adapt the training regiment to suit the patient's level of effort and ability but have a limited range of motion [22]. Other configurations include dual Stewart platforms [23], or controlled trajectories with a patient lying in a reclined posture [24,25]. Stewart platforms' have limited ability in providing the range of motion needed for full gait training and reclined-posture robots control schemes surround only trajectory-based exercise.

Improving motivation and engagement of patients is another potential for robotic systems to augment the rehabilitation process. Virtual environments and haptic devices provide customized, targeted, and engaging interventions with patients [26]. Customized tasks and/or game-like scenarios suited to the patients' needs have already been used in upper extremity robotic rehabilitation [9,8,27]. Gait training devices have been slow to adopt virtual environments and haptic control likely because of the high loading requirements, a large workspace for leg interaction, and a strong focus on only walking trajectories. Development with the HapticWalker includes force control strategies for its use as a haptic platform [28], but does not incorporate visualizations, and is limited to virtual treadmills and stairs. Some studies with LOPES and Lokomat have investigated the application of virtual environments accompanying treadmill walking [29,30] but cannot be generalized for other activities or exercises.

It is clear that the complexity in the gait rehabilitation process elicits a multitude of design approaches motivated by different challenges and interpretations of the needs of patients and therapists. The efficacy of the various controller implementations, configurations and actuation systems are difficult to assess and there is still a lack of widespread randomized clinical trials for motivating clinical adoption of gait rehabilitation robots [31,32]. Initial clinical trials with the Lokomat conclude that it is not more effective than conventional overground therapy techniques [33,34]. The versatility and programmability of a robotic device can be further embraced with a robotics system that has the capacity to provide a greater breadth of exercise regiments closely linked to current practices in the clinic for therapists to administer rather than designing a device based on a specific functionality or control scheme.

The following sections describes the ViGRR prototype design cycle from requirements analysis to the details of mechanical and controller design, and conclude with user-driven experiments conducted to evaluate the prototype's functionality.

2. Conceptual design

2.1. Functional requirements

Lower-extremity robotic devices employ trajectory based exercises, involve large upright platforms, and are not currently designed to tailor to the variability, specificity and flexibility of exercises administered by therapists in a clinical setting [35,9]. There is a need to implement a safe interactive robotic platform with underlying technologies that can not only train predefined trajectories, but also employs a number of targeted exercise tasks with virtual environments. Early intervention for post-stroke victims is key to optimal functional recovery and the ability to use a robotic platform in a supine position for acute stroke patients would provide a beneficial opportunity for reaching patients who would otherwise be sedentary [25]. The functional requirements for a gait rehabilitation robot should include: (A) Perform as a haptic display with visual and force feedback; (B) Support the legs and the foot such that exercises and interactions beyond average gait trajectories can be implemented; (C) Provide a range of torso configurations from simple exercises in a supine configuration to fully upright for gait trajectories; (D) Measure patient joint kinematics and dynamics for assessment and monitoring; and (E) Is compact, safe, easy to don and doff, accommodate a wide range of patients within the stroke population, and be operated by one or two therapists.

2.2. ViGRR concept

The ViGRR concept prototype is envisioned as a robotic device that interfaces with a patient's lower extremities and acts as a haptic interface for virtual exercises relevant to gait rehabilitation. Fig. 1 shows the prototype of the ViGRR concept with a manipulator for the right leg. ViGRR differentiates itself from other gait rehabilitation robots by introducing flexible task-based gaming environments for the lower extremities in a format accessible for low-functioning or even bed-ridden patients yet powerful enough to provide a portion of ground reaction forces expected from the normalized gait trajectories.

The required high-level operational framework for the ViGRR is provided in Fig. 2 involving three distinct processes: *Assessment*, *training*, and *control*. The concept includes real-time patient assessment measurements and therapist inputs to generate a desired physics-based game or task with haptic rendering and sensory feedback. The robot controller then matches the desired force or trajectory generated by the haptic interaction of the robot with the virtual environment.

For example, if a physiotherapist treats ankle dorsiflexion of patient having difficulty reacting to obstacles on their left (left neglect), they can set up a gaming environment that requires attention on the left side of the screen and incorporates an activity that challenges the patient to flex their ankle. Other potential exercises may focus on: balancing a ball on a virtual plank (balance recovery); football kick (hip flexor strengthening); pushing each foot to steer a race car (weight shift training); and altering leg press movements according to musical or visual cues (improving symmetrical muscle activations and timing). The ViGRR platform could provide many types of activities that target specific functional gains with the added benefits of autonomous operation, improved safety, fewer space and equipment requirements, detailed measurements of the patient's effort, real-time feedback, and reduced physical burden on the therapist.

The ViGRR prototype is realized as a planar 4DoF all-revolute serial manipulator with a force/torque sensor at the end effector

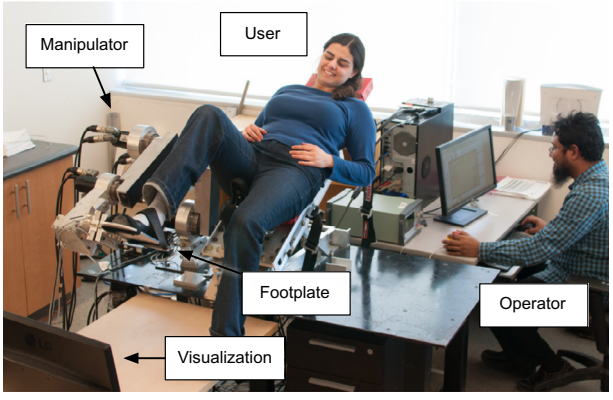

Fig. 1. Overview of the ViGRR prototype.

Please cite this article in press as: Chisholm KJ et al. A task oriented haptic gait rehabilitation robot. Mechatronics (2014), http://dx.doi.org/10.1016/j.mechatronics.2014.07.001

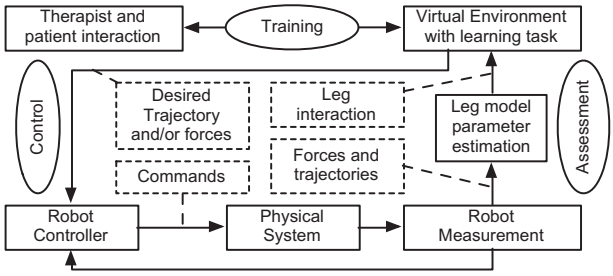

Fig. 2. ViGRR controller concept flow chart.

which interfaces with a user's foot. The torso is fixed to a reclined seat with an adjustable back rest and the footplate is offset from the linkages of the manipulator. The decided configuration of the robot features: (A) A *serial manipulator* with the base joint at the user's hip was chosen to act as an analogue to the lower extremities accommodating an appropriate workspace for multiple torso angles. (B) The planar robot is *offset to the side of the user*, with a detachable foot plate constrained to move only in the sagittal plane. This prevents collisions between the user and the robot, and allows for a quick mechanical release of the leg in case of emergency. (C) There is a single human-robot physical connection with requiring only a single force sensor for the foot and does not require adjustable linkage lengths for the manipulator. (D) The *redundant 4-DOF serial manipulator* adds robustness and flexibility to the system, however optimization is required for inverse kinematics.

3. Requirements analysis

The performance requirements of the ViGRR platform are largely based on a person's gait, considering ambulation is a desirable functional outcome for gait rehabilitation. An analysis of average gait trajectories with a simplified leg model was chosen for generating required workspace loading requirements which were then used with a robot simulation to optimize parameters in the detailed design of the robot.

3.1. Leg model

Basic assumptions of rigid bodies, bulk joint torques and revolute joint constraints were made consistent with planar gait analysis biomechanics modeling [36,37] and were implemented in simulations required for the detailed iterative design process.

The leg model is analogous to a serial 3R robotic arm where each leg segment (thigh, lower leg, and foot) is assumed to be a rigid body with the torso stationary and fixed to the seat (base frame {0}). Fig. 3 shows a schematic of the leg and robot model depicted separately for clarity with the thigh, lower leg and foot rigid bodies shown for the leg. The leg joint angles are denoted by θ. The foot position and orientation of the coordinate frame at the end of the foot relative to the base frame is denoted by X_h. The equations of motion for the leg model were derived using Euler–Lagrange formulation of dynamics for an all-revolute planar 3DoF manipulator and verified with the iterative Newton–Euler formulation [38].

The properties of each rigid body segment are related to the total body height (stature) of an individual and the total body weight using anthropomorphic data from studies involving cadavers and human subjects [39,37]. These length and mass proportions provide approximations when measured segment properties of the individual are not available [37] and also serve as a design tool where only a person's weight and height are required to specify the dynamic properties of the leg model.

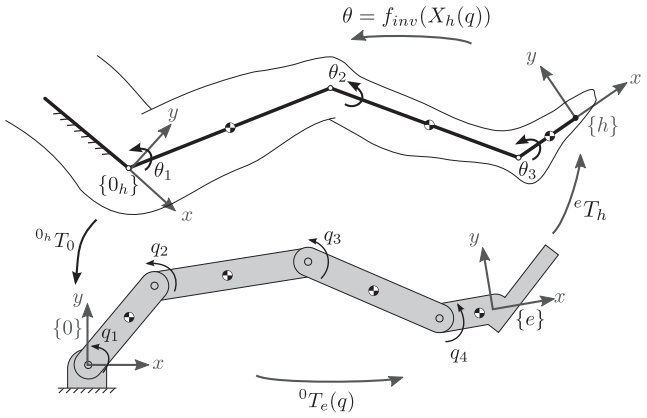

Fig. 3. Leg (top) and robot (bottom) schematics and coordinate transformations.

For use with the ViGRR human leg model, average experimental sagittal plane gait trajectories and ground reaction forces of healthy adults were obtained from [36]. A passive joint torque model was also applied to mimic passive restoring torques from soft tissues deforming and involuntary co-contractions over the joint as it approaches biological limits [40]. Fig. 4 shows the joint torque data as circle markers and the fitted spline fit and the broken line represents the bounds of one standard deviation from the mean for the collected data.

3.2. Workspace

The required workspace of the robot should accommodate a large range of body types as well as a large range of motion of the leg joints, so that a variety of exercises and tasks like walking, stair climbing and cycling can be accomplished. Joint angle limits and passive joint torque model from [40] are used with torque limits to help define the required workspace boundary. The leg model inverse kinematics were applied at foot locations and orientations

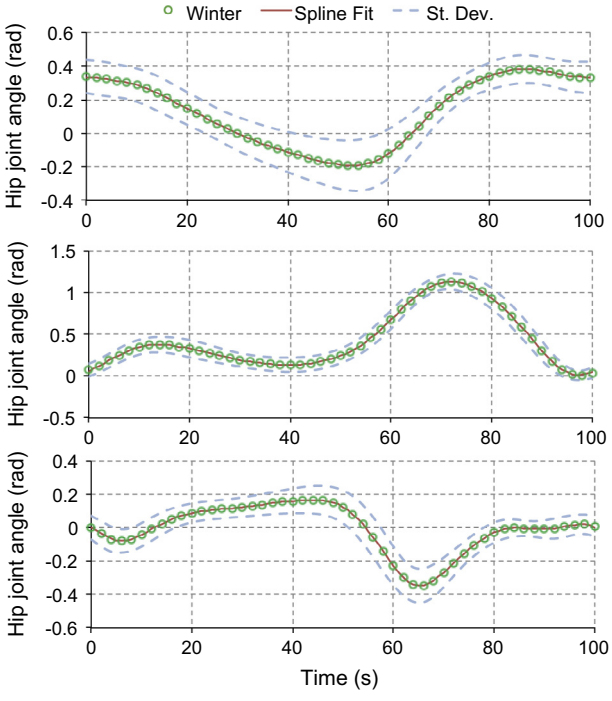

Fig. 4. Hip knee and ankle joint angles vs. percent gait cycle.

Please cite this article in press as: Chisholm KJ et al. A task oriented haptic gait rehabilitation robot. Mechatronics (2014), http://dx.doi.org/10.1016/j.mechatronics.2014.07.001

in the Cartesian space with a grid of points tested at 1 cm intervals for the position and one degree intervals for the orientation. The range, maximum, and minimum permissible foot angles were calculated within specified passive torque or joint limits. Contour plots of the leg models' workspace are presented in Fig. 5 for individuals with a height of 1.507 m and 1.887 m which correspond to 5th percentile and 95th percentile statures of American adults [41]. These two body heights and associated anthropometric limb segment lengths represent the maximum and minimum heights of individuals intended for use with the ViGRR prototype.

3.3. End effector loading requirements

From the leg dynamic model, including average gait trajectories, a passive joint torque model and anthropometric relationships, the end effector loading requirements can be calculated based only on the cadence and chosen height and mass of the individual(s). The process for determining the loading and trajectory requirements of the end effector is as follows:

1. Determine leg model parameters from height and mass of individual with anthropometric relationships.
2. Calculate average leg passive joint torques, applied bulk torques, angular positions, velocities, and accelerations from desired cadence and experimental gait data.
3. End effector positions, velocities and accelerations calculated from forward kinematics.
4. Joint torques, positions, velocities and accelerations are used in the leg's equations of motion to obtain the end effector forces and torques.

Four sets of end effector trajectories and loading requirements were generated based on walking at 100 steps per minute with 60% of the average applied leg joint torques and leg properties derived from 0° and 30° (supine) torso angles which correspond to the most extreme configurations of the user in terms of high loading requirements due to the effect of gravity and the extra support required to keep the robot and leg horizontal.

4. Manipulator design optimization

The knowledge of the system kinematics, dynamics, and loading are required to select the actuators. The choice of actuators also affects the robot parameters. For redundant robots, an intimate knowledge of optimal redundancy resolution schemes and controllers is crucial to the design process. An iterative optimization process, shown in Fig. 6, was set up to find the optimum design configuration including parameters and actuator specifications (lengths, masses, torques, speeds, transmissions, etc.) The details of modules used in the design process are highlighted in the following sections.

4.1. Robot model

The dynamic model of the ViGRR prototype was derived, a serial 4DOF manipulator, was derived analytically, which takes the form of

$$\tau = M(q)\ddot{q} + C(q,\dot{q})\dot{q} + g(q) + B\dot{q} + T_c(\dot{q}) + J^T f_e, \quad (1)$$

$\tau \in \mathbb{R}^4$ is the vector of joint torques and $q \in \mathbb{R}^4$ is the vector of joint angles. The matrix $M(q) \in \mathbb{R}^{4\times4}$ is the inertia matrix and $C(q,\dot{q}) \in \mathbb{R}^4$ is the vector of coriolis and centripetal terms. The vector $g(q) \in \mathbb{R}^4$ is associated with the effect of gravity, B is a diagonal matrix of viscous friction coefficients, $T_c(\dot{q})$ is a tanh coulomb friction model, and the robot Jacobian transpose $J^T \in \mathbb{R}^{4\times3}$ relates the static planar interaction forces applied at the end effector $f_e \in \mathbb{R}^3$ relative to frame {0} to the torques applied by the robot. The position and orientation of the robot end effector frame $\{e\}$ is denoted by $X_e \in \mathbb{R}^4$.

Thus far, we have considered the leg and robot to be separate entities, but rigidly connected. The coordinate transforms between the foot and robot are depicted in Fig. 3. A coordinate transformation, ${}^eT_h$, specifies the displacement and angle offset between the robot end effector frame $\{e\}$ and the foot coordinate frame $\{h\}$. Given the inverse kinematics of the leg model $f_{inv}(X_h)$, the joint angles can be estimated using the robot sensors.

Due to its redundancy, the inverse kinematics for ViGRR manipulator requires an optimization routine to determine a single joint configuration for a given end effector pose. Penalty functions, $\omega_l(q)$

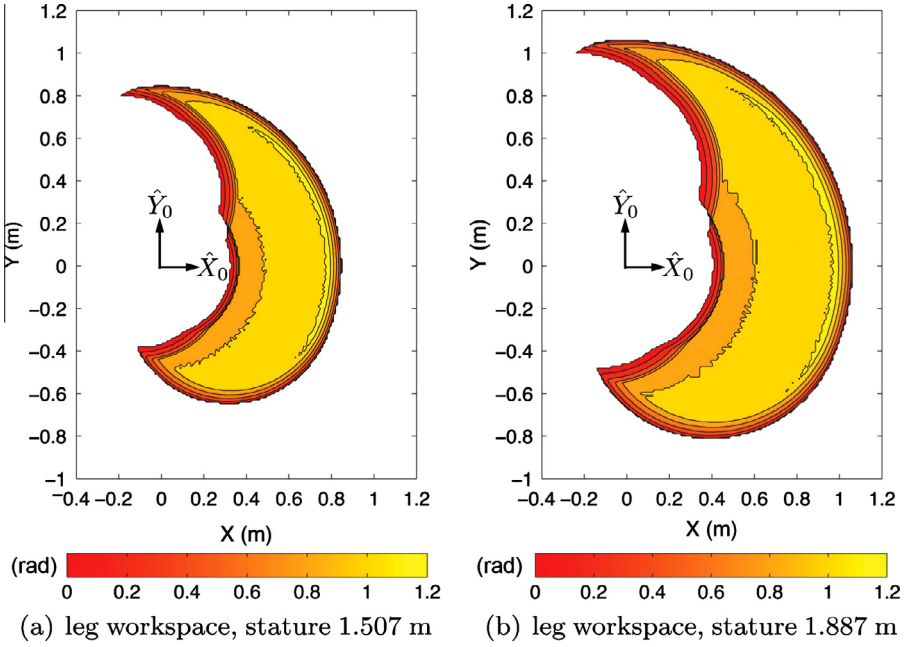

(a) leg workspace, stature 1.507 m (b) leg workspace, stature 1.887 m

Fig. 5. Leg model workspace bounds for individuals of average limb proportions and statures of 1.507 m (a) and 1.877 m (b) with contours showing the range of angles at the end effector (foot).

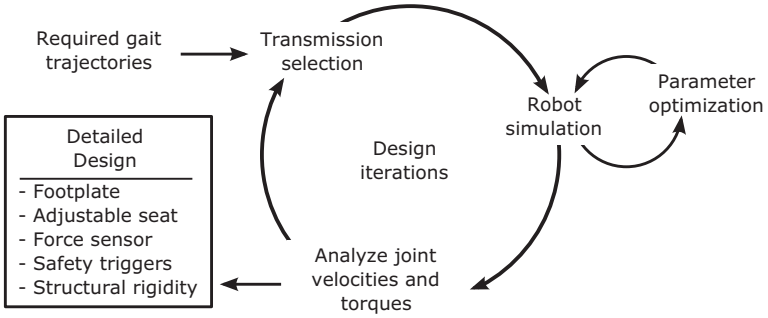

Fig. 6. Overview of the detailed design process for ViGRR.

and $\omega_s(q)$, are combined to avoid joint limits, singular configurations in finding an optimal configuration, q^*, which solves:

$$\min\{\omega(q) = k_l\omega_l(q) + k_s\omega_s(q)\} \quad \forall\ \{q \in \mathbb{R}^4 : q_{i,min} < q_i < q_{i,max}\}, \tag{2}$$

where $q_{i,min} \in \mathbb{R}^4,\ q_{i,max} \in \mathbb{R}^4$ are the joint limits for each joint i, and $k_l \in \mathbb{R},\ k_s \in \mathbb{R}$ scale the penalty functions

$$\omega_l(q) = \sum_{i=1}^{4}\left(\frac{q_i - 0.5(q_{i,max} + q_{i,min})}{q_{i,max} - q_{i,min}}\right)^2, \tag{3}$$

and

$$\omega_s(q) = -\sqrt{\det\left(JJ^T\right)}. \tag{4}$$

In order to maintain the end effector pose, the solution is optimized by applying the gradient of the objective function (2) projected to the Jacobian null space, such that

$$q^*_{k+1} = q^*_k - (I - J^{\dagger}J)\nabla\omega(q^*_k), \tag{5}$$

for iteration $k+1$ and the gradient $\nabla\omega(q^*_k)$ is determined analytically. The optimal solution converges when $\Delta q^* = q_{k+1} - q_k$ reaches a specified tolerance.

ViGRR's differential inverse kinematics employ the Jacobian pseudoinverse $J^{\dagger}$ to minimize the norm of q for a given velocity of the end effector $\dot{X}_e$ such that $\dot{q} = J^{\dagger}\dot{X}_e$ and $\ddot{q} = J^{\dagger}(\ddot{X}_e - \dot{J}\dot{q})$ [38].

4.2. Component selection and optimization

The model of the robot was used to find the motor joint torques and velocities for each set of end effector loading requirements through the design iterations. For each set iteration of the drive-train component selections (large loop in Fig. 6), their dynamic properties were applied in a simulation to find the optimal value for the design parameter defined by

$$v = [l_1\ l_2\ l_3\ l_4\ k_s\ k_l\ \psi_{eh}]^T, \tag{6}$$

where $\{l_1, l_2, l_3, l_4\}$ are the linkage lengths, and ψ_{eh} is the end effector offset angle from the foot. The optimal design parameters are found solving the optimization problem

$$\min\{f(v) = f_{rms} + 0.5f_{max}\} \quad \forall\ \{v \in \mathbb{R}^7 : v_{i,min} < v_i < v_{i,max}\}, \tag{7}$$

where $v_{i,min},\ v_{i,max}$ are the limits for each parameter in v,

$$f_{rms} = \sqrt{\frac{1}{4n}\beta(\tau(v)\tau^T(v))},$$

$$f_{max} = \beta\ \max_j|\tau_{i,j}|,$$

and $\tau(v) \in \mathbb{R}^{4\times n}$ is the matrix of calculated joint torques based on: the design parameters v, n data points from desired end effector trajectory j, and the dynamic model of the robot (1). The objective function $f(v)$ is a sum of the root mean square values of the joint torques and the maximum absolute value of each joint over the trajectory, both weighted by the vector $\beta \in \mathbb{R}^{1\times 4}$.

The objective function (7) was used with a genetic algorithm, implemented in MATLAB, to find the global optimum design vector v. A nonlinear inequality function was also created that marked the function parameters as invalid if all points on the trajectory were not reachable or the specified joint limits of ±140° were exceeded. The resulting parameters from the genetic algorithm optimization for ViGRR are provided in Table 1.

The final compatible parameters optimized by the genetic algorithm with the chosen motor and harmonic drive units provided an acceptable solution to the optimization problem. Danaher Motion AKM series DC motors and S200 drive units were selected with CSF and CSG series harmonic drives for the joint transmissions with the nominal (subscript n) and peak (subscript p) torques and velocities specified in Table 2.

4.3. Safety mechanisms and end effector design

For powerful human-interactive robots such as ViGRR, safety is paramount due to potential risks arising from collisions, moving outside comfortable bounds of a patient's range of motion or interaction forces. One key method used here, is to ensure user safety by releasing the user from the robot and ensuring that the workspace remains collision-free from the user afterwards. The footplate is magnetically attached and can be released on demand to mitigate safety risk, e.g., power loss, emergency button pressing, or controller safety limits. Fig. 7 shows the end effector in the disengaged position. Emergency stop buttons are available for the user and the therapist. A safety monitoring subsystem, in the real-time controller, monitors the configurations, velocities, forces, and torques, in both joint space and task spaces, and detects if any of the quantities exceed specified safety limits. In addition, hardware joint limit switches inhibit the drive motion to prevent damage and self collision. An important safety feature is based on estimating the patient's joint angles during the robot's operation and limiting those motions to patient-specific ranges during the operation.

5. Control system design

The final design phase for the ViGRR prototype is the development of the control hardware, architecture, and algorithms. The control architecture, shown in Fig. 8, uses a nonlinear inverse

Table 1
Nonlinear optimization results for design parameters.

l_1	l_2	l_3	l_4	k_s^0	k_l^0	ψ_{eh}
0.20	0.34	0.27	0.15	0.096	0.016	0.58

Table 2
Drive component specifications.

Joint	τ_n (N m)	τ_p (N m)	ω_n (rad/s)	ω_p (rad/s)
1	254	892	2.62	5.24
2	281	892	2.18	5.24
3	90	309	2.29	4.91
4	57	191	3.67	8.38

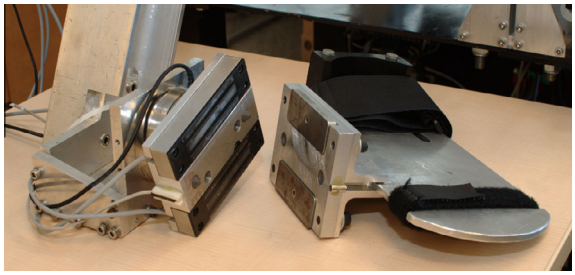

Fig. 7. End effector footplate.

dynamics task-space trajectory controller together with an impedance model and a virtual environment to enable a foot-haptic controller.

The real-time control hardware and software are implemented using a custom architecture, including a host Windows PC with Simulink and QuaRC software and a target PC with QNX real-time operating system running at 2000 Hz, interfaced with a Quanser Q8 data acquisition card. The 6-axis ATI Mini85 force/torque sensor mounted at the end effector measures the interaction forces felt by the patient. The patient seat is adjustable from 0° to 90°, allows for unhindered leg movement using a bike-style seat, and is able to slide along the direction of the patient's torso which provide various configuration for future clinical studies.

5.1. Robot controller

Feedback linearization (or inverse dynamics) trajectory control is applied to the ViGRR platform [38] resulting in a linear closed-loop system. A regressor-parameter formulation was derived in order to provide a linearized set of dynamic parameters that can be calibrated experimentally. The equations of motion can be rearranged to involve a regressor matrix $Y(q,\dot{q},\ddot{q})$ as a function of the joint positions, velocities and accelerations and a parameter vector ϕ containing the dynamic parameters. The parameter and regressor are equivalent to the robot dynamics as in

$$\begin{aligned}\tau &= M(q)\ddot{q} + C(q,\dot{q})\dot{q} + g(q) + B\dot{q} + T_c(\dot{q}) \\ &= Y(q,\dot{q},\ddot{q})\phi.\end{aligned} \tag{8}$$

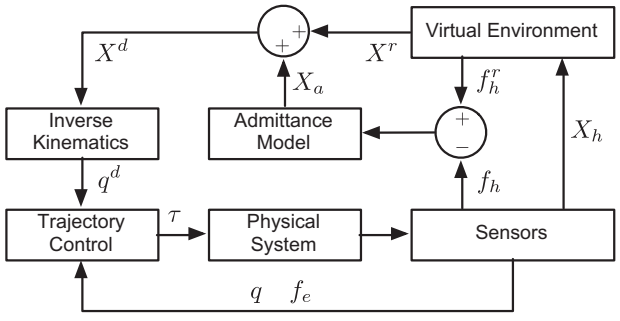

Fig. 8. Overview of ViGRR controls implementation.

The inverse dynamics controller is applied to the ViGRR trajectory controller in the form of

$$u = Y(q,\dot{q},a_q)\phi, \tag{9}$$

where u is the commanded motor torques and a_q is the new controller input. A joint space tracking proportional-derivative (PD) controller with an acceleration feedforward term is specified as

$$a_q = \ddot{q}^d + K_1\dot{\tilde{q}} + K_0\tilde{q}, \tag{10}$$

where the superscript d denotes the desired trajectory, $\tilde{q} = q^d - q$ and $\dot{\tilde{q}} = \dot{q}^d - \dot{q}$ are the joint position and velocity errors, respectively, and the positive diagonal matrices K_0 and K_1 specify the position and velocity gains for each joint.

The ViGRR robot relies on a model-based control and a calibration is required to ensure the model parameters provide the desired stable behaviour of the robot with good tracking performance. The dynamic parameter ϕ from the regressor-parameter formulation of the dynamics (8) is determined from the calibration procedure. The calibration is based on a set of trajectories for all of the joints with varying amplitudes and frequencies. The joint positions and applied torques were logged and a zero-phase filtering was performed on the joint angles to calculate the velocities and accelerations by numerical differentiation [42]. From n data points over the calibration trajectory, the dynamic parameters are determined from an augmented matrix defined by

$$\begin{aligned}&\tau = \mathbf{Y}\phi \\ &\begin{Bmatrix}\tau_1\\ \tau_2\\ \vdots\\ \tau_n\end{Bmatrix} = \begin{bmatrix}Y(q,\dot{q},\ddot{q})_1\\ Y(q,\dot{q},\ddot{q})_2\\ \vdots\\ Y(q,\dot{q},\ddot{q})_n\end{bmatrix}\phi\end{aligned} \tag{11}$$

The dynamic parameter was calculated by a least squares solution from

$$\hat{\phi} = (\mathbf{Y}^T\mathbf{Y})^{-1}(\mathbf{Y}^T\tau). \tag{12}$$

5.2. Admittance force control

In the admittance control scheme, the input is the difference between the measured force f_h and the reference (desired) force f_h^r, and the output is the error trajectory generated, using a desired impedance model, as a disturbance to the reference trajectory with a discrete-time integration process. The desired impedance model is defined as

$$(f_h - f_h^r) = M_a\ddot{\tilde{X}}_a + B_a\dot{\tilde{X}}_a + K_a\tilde{X}_a, \tag{13}$$

where $\tilde{X}_a = (X_h^d - X_h^r)$, $\dot{\tilde{X}}_a = (\dot{X}_h^d - \dot{X}_h^r)$, and $\ddot{\tilde{X}}_a = (\ddot{X}_h^d - \ddot{X}_h^r)$ are the errors in the Cartesian space and superscript r refers to a reference trajectory, subscript a refers to the disturbance trajectory generated from the impedance model and superscript d refers to the desired trajectory generated for the trajectory PD control. The terms M_a, B_a and K_a are the inertia, damping and stiffness coefficients that define the task space impedance model dynamics.

The admittance disturbances are generated using the following state-space model:

$$\begin{Bmatrix}\tilde{X}_a\\ \dot{\tilde{X}}_a\\ \ddot{\tilde{X}}_a\end{Bmatrix}_{k+1} = \begin{bmatrix}I & t_sI & 0\\ 0 & I & t_sI\\ -M_a^{-1}K_a & -M_a^{-1}B_a & 0\end{bmatrix}\begin{Bmatrix}\tilde{X}_a\\ \dot{\tilde{X}}_a\\ \ddot{\tilde{X}}_a\end{Bmatrix}_k + \begin{bmatrix}0\\ 0\\ M_a^{-1}\end{bmatrix}(f_h - f_h^r), \tag{14}$$

where t_s is the controller step size in seconds. The reference force f_h^r for the admittance controller is calculated from a virtual coupling

haptic rendering algorithm [43] that uses a 3D graphics rendering engine and rigid collision model. The virtual coupling and admittance dynamic parameters are experimentally tuned to ensure stable behaviour of the system when dealing with unpredictable haptic user interaction.

6. Preliminary experiments

Initial experiments are defined to assess the novel capabilities of ViGRR and whether it can be used for rehabilitation and human interaction as a haptic device using force feedback from a virtual environment. All the presented experiments were performed under an ethics approval from Research Ethics Board at Carleton University project 11-1631.

6.1. User driven experiments

Two main experiments were performed: A gait trajectory following to enhance the user's ability in leg swinging motion, and a targeted leg press activity to enhance sit-to-stand and balance abilities.

In the gait trajectory following the user tracks an average gait trajectory, shown on the screen, using their feet. The purpose of this experiment is to determine whether the user can follow a tracking task when the robot is in force-controlled mode. In an effort to provide a comfortable position for the user, both the seat and the reference trajectory are rotated 20°.

The impedance model was set to provide resistance to the motion with a specified viscous damping coefficient, zero stiffness, and a point mass. Fig. 9 shows the experimental setup. The user was asked to follow a reference gait trajectory with a cadence of 7.5 $\frac{steps}{min}$. Markers depicting the measured and desired positions of the foot were overlaid on the visualization with the reference trajectory for the user to follow.

Fig. 10 shows the desired and measured planar foot positions for the cyclical foot trajectory experiment performed with a healthy participant. The desired trajectory provided as visual feedback is depicted as a dashed line and the measured trajectory of the foot X_h is the solid line.

The second experiment with a virtual reality exercise environment simulates a weighted leg press which provides strength training and coordination for sit-to-stand motion with a patient. The user pushes on a weight by extending their leg in the horizontal direction, while a virtual gravity is acting on the simulated mass in the opposite direction. This weight, shown as the grey box in Fig. 11, can be varied depending on the strength of the patient. A weak patient can start with a small load which gradually increases as they progress. A leg press was performed with a healthy participant and masses of 5 kg and 10 kg at $g = 9.81$ m/s^2. Fig. 12 shows the desired and measured horizontal interaction forces relative to the global frame {0} with the virtual leg press exercise.

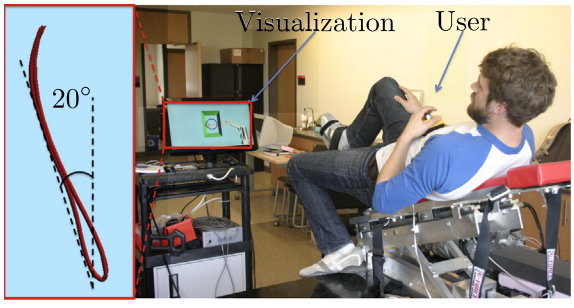

Fig. 9. Diagram of the setup for the gait trajectory following experiment.

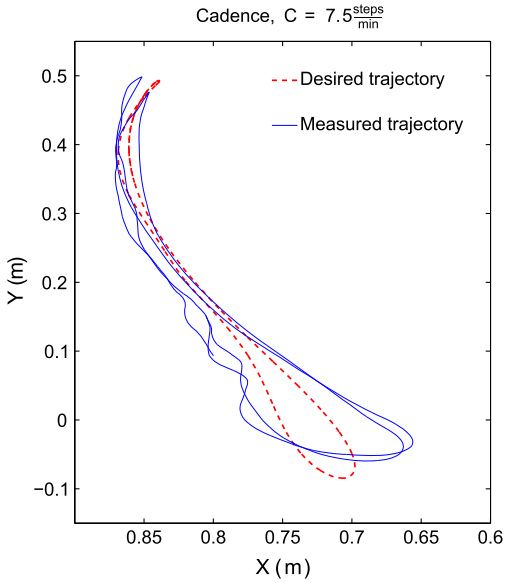

Fig. 10. Desired and measured gait trajectories during two trials for a cadence of 7.5 $\frac{steps}{min}$.

6.2. Discussion

The force feedback control scheme was successfully implemented to allow the user to track a desired path. The user demonstrated the capability of ViGRR to provide force and visual feedback to perform a motor task. The tracking plot from Fig. 10 shows the user's attempt to follow a desired foot trajectory. The user deviates from the desired trajectory near the bottom where more force is required to accelerate. Table 3 lists the dominant characteristics of the forces applied during free motion of the leg.

The noticeable oscillations in the force and position may be attributed to modeling errors from the nonlinear characteristics and the inherent flexibility of harmonic drives. An improved model of the system may provide more precise control and may reduce oscillations. Moreover, the foot-robot coupling is not rigid, and the sensory feedback and motor control of the user, who is in the loop, can also introduce oscillations. Lower viscous damping did result in larger controller oscillations and was not comfortable for the user and higher damping increases the user's effort and decreases the robot's transparency.

The leg press experiment demonstrated not only a visual feedback and interactive experience with the user, but also incorporated haptic feedback driven by the physics-based gaming environment. The applied forces from the user are relatively noisy

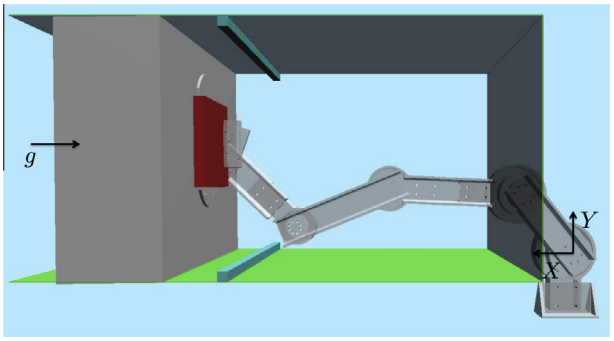

Fig. 11. Leg press exercise with ViGRR where the patient pushes in the X direction, acting against gravity. The large and small boxes represent the weight and virtual tool respectively.

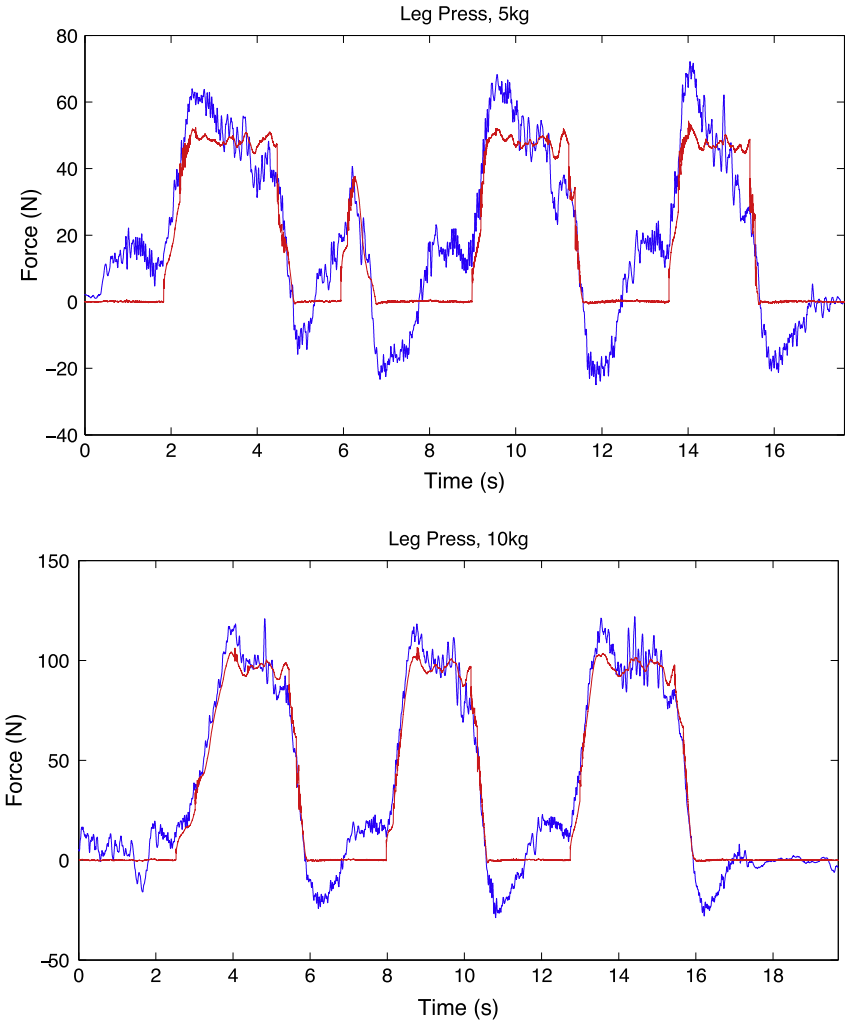

Fig. 12. Leg Press experiment for a 5 kg (top) and 10 kg (bottom) weight. The blue line represents the measured forces at the FT sensor and the red line represents the haptic interaction forces. (For interpretation of the references to colour in this figure legend, the reader is referred to the web version of this article.)

Table 3
Force characteristics for gait trajectory following task.

Parameter	Value	Units
M_a	[10,10,1]	(kg, kg, N m^2)
B_a	[55,55,10]	(N s/m, N s/m, N s/rad)
K_a	[0,0,30]	(N/m, N/m, N m/rad)
f_h^r	[0,0,0]	(N, N, N m)
t_s	1/2000	s

and exhibit more prevalent oscillations compared to the reference forces from the haptic rendering. This discrepancy may be caused by structural or physical dynamic interactions and/or motor control artifacts. Further refinement and detailed characterization of the haptic performance and stability should be performed in future investigations.

The intended application of the ViGRR prototype and these experiments is to demonstrate its rehabilitation-focused capabilities. We can look at the initial controller concept flow chart in Fig. 2 and refer to analogous portion of the virtual environment tasks in order to elucidate its application to gait training. In the *training* portion of the controller, the trajectory following task incorporates task space dynamics that include damping, stiffness and inertia terms of the impedance model. The leg press incorporates direct interaction with a physical mass and virtual gravity. Training and interactive feedback to the user is in the form of a 3D graphic visualization and force feedback. The *controller* portion of the control scheme tracks the desired output from the virtual environment or admittance control process. In the *assessment* portion of the controller concept, the user's effort is measured by the force/torque sensor and their tracking performance is also assessed by inspecting the task space reference trajectory and measured foot positions as shown in Fig. 10. ViGRR's ability to measure or estimate different variables is an asset that can lead to further study into controllers or tasks that provide different types of information as feedback to the user and therapist that are relevant to the task in the virtual environment.

7. Conclusion

It was shown that ViGRR is capable of operating as a haptic device for rehabilitation applications and provide repetitive exercises in an effort to improve functional outcomes for the lower extremities. A full mechatronics system was conceived, designed, calibrated and tested with it's intended application. Further investigation and development of the platform's technical capabilities will inform future virtual environments for gait rehabilitation tasks and ultimately, experiments with stroke patients.

Please cite this article in press as: Chisholm KJ et al. A task oriented haptic gait rehabilitation robot. Mechatronics (2014), http://dx.doi.org/10.1016/j.mechatronics.2014.07.001

References

[1] Dobkin BH. Strategies for stroke rehabilitation. Lancet Neurol 2004;3(9):528–36.
[2] Lindsay P, Bayley M, McDonald A, Graham ID, Warner G, Phillips S. Toward a more effective approach to stroke: Canadian best practice recommendations for stroke care. CMAJ 2008;178(11):1418–25.
[3] Daniel K, Wolfe CDA, Busch MA, McKevitt C. What are the social consequences of stroke for working-aged adults? A systematic review. Stroke 2009;40(6):e431–40.
[4] Behrman AL, Bowden MG, Nair PM. Neuroplasticity after spinal cord injury and training: an emerging paradigm shift in rehabilitation and walking recovery. Phys Ther 2006;86(10):1406–25.
[5] King A, McCluskey A, Schurr K. The time use and activity levels of inpatients in a co-located acute and rehabilitation stroke unit: an observational study. Top Stroke Rehabil 2011;18(Suppl. 1):654–65.
[6] Askim T, Bernhardt J, Lge AD, Indredavik B. Stroke patients do not need to be inactive in the first two-weeks after stroke: results from a stroke unit focused on early rehabilitation. Int J Stroke 2012;7(1):25–31.
[7] Belda-Lois J-M, Mena-Del Horno S, Bermejo-Bosch I, Moreno JC, Pons JL, Farina D, et al. Rehabilitation of gait after stroke: a review towards a top-down approach. J Neuroeng Rehabil 2011;8(1):66.
[8] Hesse S, Schmidt H, Werner C, Bardeleben A. Upper and lower extremity robotic devices for rehabilitation and for studying motor control. Curr Opin Neurol 2003;16(6):705–10.
[9] Marchal-Crespo L, Reinkensmeyer DJ. Review of control strategies for robotic movement training after neurologic injury. J Neuroeng Rehabil 2009;6:20.
[10] Visintin M, Barbeau H, Korner-Bitensky N, Mayo NE. A new approach to retrain gait in stroke patients through body weight support and treadmill stimulation. Stroke 1998;29(6):1122–8.
[11] Colombo G, Wirz M, Dietz V. Driven gait orthosis for improvement of locomotor training in paraplegic patients. Spinal Cord 2001;39(5):252–5.
[12] West G. Powered gait orthosis and method of utilizing same. US Patent 6689075; 2004.
[13] Freivogel S, Schmalohr D, Mehrholz J. Improved walking ability and reduced therapeutic stress with an electromechanical gait device. J Rehabil Med 2009;41(9):734–9.
[14] Riener R, Lunenburger L, Jezernik S, Anderschitz M, Colombo G, Dietz V. Patient-cooperative strategies for robot-aided treadmill training: first experimental results. IEEE Trans Neural Syst Rehab Eng 2005;13(3):380–94.
[15] Banala SK, Agrawal SK, Scholz JP. Active leg exoskeleton (alex) for gait rehabilitation of motor-impaired patients. In: Proc IEEE 10th international conference on rehabilitation robotics ICORR 2007; 2007. p. 401–7.
[16] Banala SK, Agrawal SK, Kim SH, Scholz JP. Novel gait adaptation and neuromotor training results using an active leg exoskeleton. IEEE/ASME Trans Mech 2010;15(2):216–25.
[17] Veneman JF, Kruidhof R, Hekman EEG, Ekkelenkamp R, Asseldonk EHFV, van der Kooij H. Design and evaluation of the lopes exoskeleton robot for interactive gait rehabilitation. IEEE Trans Neural Syst Rehabil Eng 2007;15(3):379–86.
[18] Stauffer Y, Allemand Y, Bouri M, Fournier J, Clavel R, Metrailler P, et al. The WalkTrainer-a new generation of walking reeducation device combining orthoses and muscle stimulation. IEEE Trans Neural Syst Rehabil Eng 2009;17(1):38–45.
[19] Schmidt H, Werner C, Bernhardt R, Hesse S, Krger J. Gait rehabilitation machines based on programmable footplates. J Neuroeng Rehabil 2007;4:2.
[20] Hussein S, Schmidt H, Hesse S, Kruger J. Effect of different training modes on ground reaction forces during robot assisted floor walking and stair climbing. In: Proc IEEE int conf rehabilitation robotics ICORR 2009; 2009. p. 845–50.
[21] Hesse S, Waldner A, Tomelleri C. Innovative gait robot for the repetitive practice of floor walking and stair climbing up and down in stroke patients. J Neuroeng Rehabil 2010;7:30.
[22] Colombo G, Schreier R, Mayr A, Plewa H, Rupp R. Novel tilt table with integrated robotic stepping mechanism: design principles and clinical application. In: Proc 9th int conf rehabilitation robotics ICORR 2005; 2005. p. 227–30.
[23] Boian RF, Bouzit M, Burdea GC, Lewis J, Deutsch JE. Dual stewart platform mobility simulator. In: Proc 9th int conf rehabilitation robotics ICORR 2005; 2005. p. 550–55.
[24] Metrailler P, Blanchard V, Perrin I, Brodard R, Frischknecht R, Schmitt C, Fournier J, Bouri M, Clavel R. Improvement of rehabilitation possibilities with the MotionMaker TM. In: Proc first IEEE/RAS-EMBS int conf biomedical robotics and biomechatronics biorob 2006; 2006. p. 359–64.
[25] Monaco V, Galardi G, Coscia M, Martelli D, Micera S. Design and evaluation of neurobike: a neurorehabilitative platform for bedridden post-stroke patients. IEEE Trans Neural Syst Rehabil Eng 2012;20(6):845–52.
[26] Holden MK. Virtual environments for motor rehabilitation: review. Cyberpsychol Behav 2005;8(3):187–211. discussion 212–9.
[27] Krebs HI, Hogan N. Therapeutic robotics: a technology push. Proc IEEE Inst Electr Electron Eng 2006;94(9):1727–38.
[28] Hussein S, Buchel M, Kruger J. Stable, adaptive interaction and contact transition control of a high inertia haptic interface for haptic simulation in gait rehabilitation. In: Proc IEEE int robotics and automation (ICRA) conf; 2011. p. 4176–81.
[29] Van Asseldonk EHF, Ekkelenkamp R, Veneman JF, Van der Helm FCT, van der Kooij H. Selective control of a subtask of walking in a robotic gait trainer(lopes). In: Proc IEEE 10th international conference on rehabilitation robotics ICORR 2007; 2007. p. 841–8.
[30] Wellner M, Guidali M, von Zitzewitz J, Riener R. Using a robotic gait orthosis as haptic display – a perception-based optimization approach. In: Proc IEEE 10th international conference on rehabilitation robotics ICORR 2007; 2007. p. 81–8.
[31] Hogan N, Krebs HI, Rohrer B, Palazzolo JJ, Dipietro L, Fasoli SE, et al. Motions or muscles? some behavioral factors underlying robotic assistance of motor recovery. J Rehabil Res Dev 2006;43(5):605–18.
[32] Hidler J, Hamm LF, Lichy A, Groah SL. Automating activity-based interventions: the role of robotics. J Rehabil Res Dev 2008;45(2):337–44.
[33] Hidler J, Nichols D, Pelliccio M, Brady K, Campbell DD, Kahn JH, et al. Multicenter randomized clinical trial evaluating the effectiveness of the Lokomat in subacute stroke. Neurorehabil Neural Repair 2009;23(1):5–13.
[34] Hornby TG, Campbell DD, Kahn JH, Demott T, Moore JL, Roth HR. Enhanced gait-related improvements after therapist-versus robotic-assisted locomotor training in subjects with chronic stroke: a randomized controlled study. Stroke 2008;39(6):1786–92.
[35] Pennycott A, Wyss D, Vallery H, Klamroth-Marganska V, Riener R. Towards more effective robotic gait training for stroke rehabilitation: a review. J Neuroeng Rehabil 2012;9:65.
[36] Winter DA. The biomechanics and motor control of human gait. University of Waterloo Press; 1991.
[37] Winter DA. Biomechanics and motor control of human movement. Wiley; 2005.
[38] Siciliano B, Sciavicco L, Villani L, Oriolo G. Robotics modelling, planning and control. Springer-Verlag London Limited; 2009.
[39] Drillis R, Contini R. Body segment parameters. Tech rep 1166 03. Office of vocational rehabilitation, department of health, education and welfare; 1966.
[40] Riener R, Edrich T. Identification of passive elastic joint moments in the lower extremities. J Biomech 1999;32(5):539–44.
[41] McDowell MA, Fryar CD, Ogden CL, Flegal KM. Anthropometric reference data for children and adults: United States, 2003–2006. National health statistics report number 10, U.S. department of health and human services; October 2008.
[42] Chisholm K. Design and control for a gait rehabilitation robot. Master's thesis, Carleton University; 2010.
[43] Ortega M, Redon S, Coquillart S. A six degree-of-freedom god-object method for haptic display of rigid bodies with surface properties. IEEE Trans Vis Comput Graph 2007;13(3):458–69.

Please cite this article in press as: Chisholm KJ et al. A task oriented haptic gait rehabilitation robot. Mechatronics (2014), http://dx.doi.org/10.1016/j.mechatronics.2014.07.001